Int J Thermophys (2009) 30:1748–1772
DOI 10.1007/s10765-009-0668-1

Techniques for Accurate Resistance Measurement in the Transient Short-Hot-Wire Method Applied to High Thermal-Diffusivity Gas

P. L. Woodfield · S. Moroe · J. Fukai · M. Fujii · K. Shinzato · M. Kohno · Y. Takata

Received: 22 April 2009 / Accepted: 16 October 2009 / Published online: 7 November 2009

Abstract The accuracy of high-speed transient resistance measurements is an important issue particularly for measuring the thermal conductivity of high thermal-diffusivity (low-density) gases. This is because the hot-wire temperature rise against the logarithm of time is non-linear and can approach a steady state within the typical measurement time of 1 s. Two types of voltmeters are compared for use in the transient short-hot-wire method. Details of suitable procedures for taking accurate transient resistance measurements with either a two-channel high-speed analog/digital converter or a pair of integrating digital multimeters are presented.

P. L. Woodfield (✉) · M. Fujii · K. Shinzato
Research Center for Hydrogen Industrial Use and Storage, National Institute of Advanced Industrial Science and Technology, 744 Mootoka, Nishi-ku, Fukuoka 819-0395, Japan
e-mail: p.woodfield@aist.go.jp

M. Fujii
e-mail: fujii-motoo@aist.go.jp

K. Shinzato
e-mail: k.shinzato@aist.go.jp

S. Moroe · M. Kohno · Y. Takata
Department of Mechanical Engineering, Kyushu University, Nishi-ku, Fukuoka 819-0395, Japan
e-mail: shogo@gibbs.mech.kyushu-u.ac.jp

M. Kohno
e-mail: kohno@mech.kyushu-u.ac.jp

Y. Takata
e-mail: takata@mech.kyushu-u.ac.jp

J. Fukai
Department of Chemical Engineering, Kyushu University, Nishi-ku, Fukuoka 819-0395, Japan
e-mail: jfukai@chem-eng.kyushu-u.ac.jp

Keywords Helium · Low-density gas · Thermal-conductivity measurement · Transient short-hot-wire method

1 Introduction

The transient hot-wire method is the widely recommended technique for measurement of fluid thermal conductivity for all regions except the critical region and the low-density gas region [1]. However, because of the practical and theoretical importance of dilute-gas thermal conductivity, some studies have been devoted to improvements and modifications to the technique so that transient hot-wire instruments can also be used for low-density/high thermal-diffusivity gases [2–5]. Application of transient hot-wire methods to high thermal-diffusivity gases presents a number of challenges because the heated region of the sample can extend to the wall of the vessel in less than 1 s [2] and the heat capacity of the wire becomes more important [3]. Therefore, to capture the details of the transient rise in temperature, a fast sampling rate is required. Moreover, the temperature rise against the logarithm of time may not have a linear section for a low-density gas, so a curve-fitting procedure is necessary to analyze the data [2]. Some alternatives are to calculate the thermal conductivity based on the steady-state temperature rise [4] or use an extremely fine wire in a large diameter cell [3].

To meet the conflicting requirements of high accuracy and a fast sampling rate, particular attention must be given to the type and configuration of the voltmeters and the data acquisition circuit. The two general approaches for measuring the resistance of the hot wire are either using a Wheatstone bridge (e.g., [4]) or a simple direct-current circuit (e.g., [6]). Integrating digital multimeters are a popular choice for voltage measurement instruments in single-wire methods such as the transient short-hot-wire method [6,7]. They are also often used in bridge circuits for the conventional two-wire method [1]. However they can suffer from a large increase in signal noise if the sampling rate is increased greatly beyond the power-line frequency (typically $50\,s^{-1}$ or $60\ s^{-1}$). Assael et al. [8] overcame this difficulty with a specially designed circuit that measured the time (within $\pm 0.1\mu s$) at which their bridge came into balance with a series of different reference voltages. Through this technique, they were able to take over 1,000 measurements in 1 s without diminishing the accuracy of individual readings. An alternative method is to use computer controlled non-integrating digital voltmeters such as was successfully done by Roder [9] and Perkins et al. [10] in their bridge circuit with a sampling rate of approximately $250\ s^{-1}$. The automatic Wheatstone bridge of Beirao et al. [11] also appears to be operated at a sampling rate of approximately $250\ s^{-1}$. Much higher speed analog/digital converters are available on the present-day market. While there are obvious advantages in terms of time resolution, the question that needs to be answered is whether or not such devices can compete with the high accuracy of integrating multimeters for voltage measurement. Ultimately, the choice of instruments should be based on the accuracy of the determined thermal conductivity.

In this study, we compare a high-quality two-channel A/D converter with a pair of integrating digital multimeters for the application of measurements of high thermal-diffusivity gas thermal conductivity. Rather than employing a bridge, a simple

direct-current circuit containing a standard resistor in series with the hot wire was used. This kind of circuit is typical for the transient short-hot-wire method [6,7]. We focus on the different issues we faced in making use of each of the instruments and the procedures that the first two authors found to be most effective for accurate transient resistance measurement.

2 Experimental Setup and General Procedures

Figure 1 shows a schematic diagram of the experimental apparatus. The platinum hot wire has a nominal diameter of 10 μm and a length of about 15 mm. Before attaching the wire, it was annealed for 3 h at 500 °C in an electric oven. Following this, it was spot welded onto two 1.5- mm diameter platinum terminals which are connected to 0.75 mm platinum leads to the four-terminal resistance measurement method. The cell design is shown in Fig. 1 and is typical for the transient short-hot-wire method [6,7]. The use of platinum material for the supporting terminals is motivated by an attempt to reduce Seebeck effects and to avoid changing the tension in the hot wire at different bath temperatures. This problem may occur if the supporting leads and hot wire were made of dissimilar materials with different coefficients of thermal expansion. The pressure vessel, which contains both the gas sample and the hot wire, has an inside diameter of 30 mm and a height of 47 mm. The gas pressure is measured by a Bourden gauge with an estimated precision of about 0.01 MPa. Before supplying the sample gas, the cell is evacuated using a vacuum pump to remove the gas from the previous experiment. The cell itself is immersed in a thermostatic bath which is capable of maintaining a steady temperature over several hours within a precision of several millikelvins. A constant current is supplied to the cell by a current source device (Keithley 2602 source meter) which is controlled by a personal computer via a General Purpose Interface Bus (GPIB) line. The transient voltage across the hot wire is measured with both a high-speed A/D converter (National Instruments PXI-5922) and an integrating digital multimeter (Keithley 2002). The current flowing through the circuit is measured simultaneously with the other channel of the A/D converter and another digital multimeter (also Keithley 2002) using a four-terminal 25 Ω standard resistor.

Rather than using a small current, two different currents (e.g., 14 mA and 7 mA) were used to determine the initial resistance of the hot wire via extrapolation to zero power (against the square of the current multiplied by the instantaneous resistance, I^2R). A somewhat similar extrapolation procedure was used by Srivastava and Saxena [12] under vacuum conditions in their steady-state hot-wire thermal-conductivity cell. In this study, the transient resistance was measured using both forward and reverse polarities and ensemble averaging was applied to the resistance measured with the larger current to reduce noise and remove the effect of the current polarity. The motivation for reversing the polarity is similar to that of Perkins et al. [10] who included a computer-driven reversing switch in their bridge circuit to remove the effect of thermal emfs in the wire and lead connections. Figure 2a shows a typical sequence of electrical currents supplied to the hot wire. Each resistance measurement has a duration (Δt_{meas}) of about 1 s with a delay (Δt_{wait}) of 15 s between consecutive measurements.

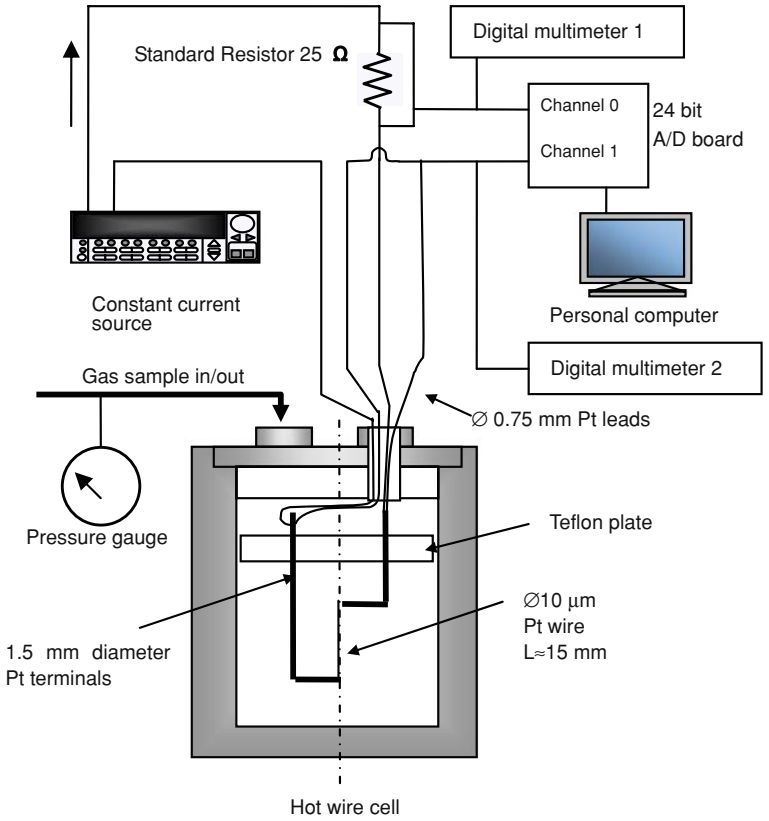

Fig. 1 Experimental setup

The polarity is reversed by sending a command to the current source to output a negative current. All instruments are computer controlled and synchronized using a LabView^{TM} computer program.

Figure 2b shows typical transient resistance measurements with the A/D converter corresponding to the currents supplied as shown in Fig. 2a. The sampling rate is 50000 s^{-1}. The bath temperature and temperature rise of the wire are determined from the measured resistances using

$$R = R_{0C}(1 + \beta T_c) \tag{1}$$

where T_c is the wire temperature (°C). The resistance at 0 °C ($R_{0C} = 19.8583\,\Omega$) and the temperature coefficient of resistance ($\beta = 0.003852\,K^{-1}$) were determined by *in situ* measurements of the hot-wire resistance and bath temperature (from 20 °C to 60 °C) with a standard platinum resistance thermometer (SPRT) which itself was calibrated according to the international temperature scale, ITS-90. In determining the volume-averaged temperature rise of the 10 μm wire, a small correction is made for

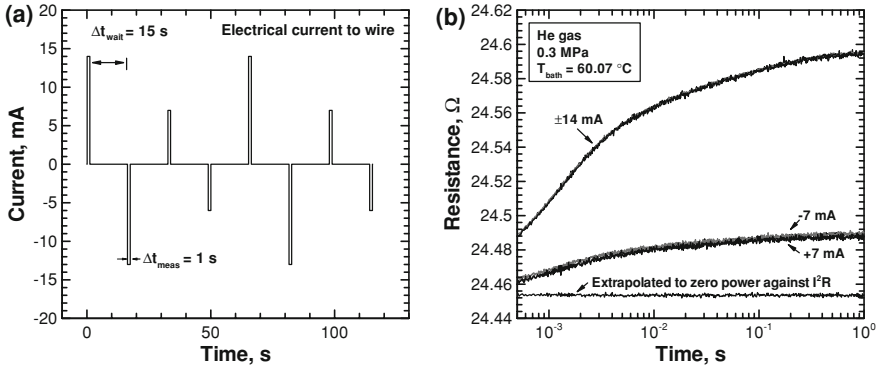

Fig. 2 Supplied currents and resistances during a single run. **(a)** Electrical current to wire and **(b)** typical resistance measurements (a negative current means a reverse in the polarity of the current source)

the resistance of the 1.5 mm diameter platinum terminals (which includes temperature dependency) [6].

3 Physical Model and Data Analysis

The transient short-hot-wire method differs from the conventional two-wire transient hot-wire method in that one wire is used and end effects are accounted for by a numerical solution of the two-dimensional unsteady heat conduction equation given by:

$$\rho c \frac{\partial T}{\partial t} = \frac{1}{r}\frac{\partial}{\partial r}\left(r\lambda\frac{\partial T}{\partial r}\right) + \frac{\partial}{\partial z}\left(\lambda\frac{\partial T}{\partial z}\right) + Q \tag{2}$$

$$\begin{aligned} Q &= q/\pi r_0^2 (r \le r_0) \\ &= 0\,(r > r_0) \end{aligned} \tag{3}$$

$$\frac{\partial T}{\partial z}|_{z=L/2} = 0 \tag{4}$$

$$T|_{r=R} = T|_{z=0} = T|_{t=0} = 0 \tag{5}$$

The heating power q, per unit length of the wire is assumed to stay constant. A symmetry boundary (Eq. 4) is applied at half the length of the wire ($z = L/2$). The temperature rise T is initially zero (Eq. 5) and the cell wall ($r = R$) and at the end of the wire ($z = 0$) are taken to be isothermal. The properties ρ, c, and λ are those of the wire for $r < r_0$ and those of the sample for $r > r_0$. Radiation heat transfer and temperature jump effects are neglected in this study.

The thermal conductivity and thermal diffusivity are determined via a least-squares curve fitting procedure such that S is minimized, as follows:

$$S = \sum_{i=1}^{N_{\text{meas}}} \left(T_{\text{calc}(i)}\,(\lambda, \alpha) - T_{\text{meas}(i)}\right)^2 \tag{6}$$

Details of the curve-fitting procedure and numerical solution of Eq. 2 are given in [2] and [13]. A somewhat complicated analytical solution [14] is also available for this problem. Since the analytical solution is more computationally expensive, routine calculations were done using the numerical procedure in [13] and verification of the accuracy of the numerical calculation was done with the analytical solution [14]. It could be confirmed that the accuracy of the numerical procedure was better than 0.1 % of the calculated temperature rise.

4 Timing and Synchronization

To obtain the correct transient change in resistance, it is of great importance to know the precise time at which the current source was started relative to the measured voltages. Assael et al. [1] observed that timing errors can be made negligible because of the high time resolution of modern timing devices. However, if the synchronization of the current source and voltmeter is incorrect then significant errors can result. Roder [15] and Watanabe [16] also noted that the performance of their transient hot-wire measurement systems was improved through giving extra attention to the timing and synchronization of the instruments. In setting up the present experiment, we found that the performance with respect to synchronization of the current source and voltmeter can be quite different depending on how the instruments are programmed. Also, treatment of the timing is different for the two types of voltmeters we are considering. Therefore, we consider it is worthwhile to discuss this issue in some detail.

4.1 Timing of A/D Converter

In the case of the high-speed A/D converter, timing is not a major issue provided the measurement is started prior to the triggering of the current source. Figure 3 shows voltages measured in the vicinity of switching on of the current source. The voltage measurement across the reference resistor (white circles) is opposite in polarity to that measured across the hot wire (black squares) due to the internal circuit design of the two-channel converter. The two channels are not completely independent since the negative terminals are internally connected to the chassis ground through two 200 Ω resistors (Note that the default setting for the negative terminals on the A/D converter is a common earth, but this is undesirable for four-terminal resistance measurement). We can see from Fig. 3 that the current source does not follow the ideal rectangular step from zero current to the constant value, but rather a small voltage appears first at about −0.25 ms before the main application of voltage ($t = 0$ ms in Fig. 3). We may suppose that initially a small current is used in the feedback circuits of the current source instrument to provide an estimate of the resistance load to supply the correct voltage corresponding to the requested current. To decide the zero point ($t = 0$ ms) in Fig. 3, a simple computer search algorithm was applied to find the measured voltage that is closest to half of the large steady voltage across the reference resistor.

With respect to accuracy of the timing, Fig. 3 shows that the ambiguity of the timing is not due to the resolution of the time sampling rate (here ±0.02 ms), but rather due to the fact that the current is supplied in a non-ideal manner (not a perfect step). Taking

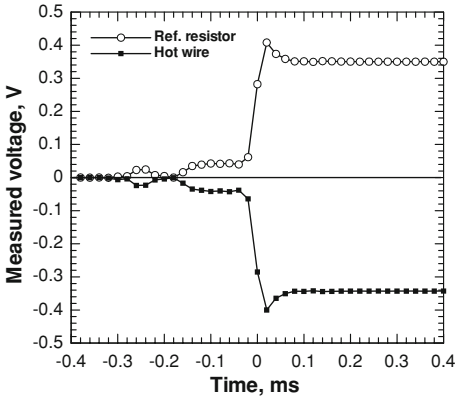

Fig. 3 Voltages measured by the A/D converter at the start of application of current to the circuit

this into account, we may suppose based on Fig. 3 that the timing error is not more than ± 0.1 ms. From the correspondence between the reference resistor and hot-wire voltages in Fig. 3, it is clear that synchronization of the two channels is at least as good as the sampling rate of ± 0.02 ms. Further improvements to the timing may be made by improving the quality of the current step. It is also worth mentioning here that the magnitude of the voltage overshoot shown in Fig. 3 can be reduced by selecting an internal "Hanning"-type filter in the programmable setup for this particular A/D converter.

4.2 Timing of Digital Multimeters

Obtaining the correct timing with the digital multimeters was considerably more difficult than the A/D converter. The reason is that the sampling rate is not fast enough to confirm the location of $t = 0$ simply by examining the measured voltages. To synchronize the current source and the two multimeters, a computer program was written using the instrument control software LabView^{TM} to follow the algorithm in Fig. 4. There are several different ways that the instruments can be programmed for synchronization. For the current source, it was found that the synchronization was more repeatable if a script program was first uploaded and then executed from within the buffer of the instrument rather than sending commands one by one along the general interface purpose bus (GPIB). Likewise for the digital multimeters, it was better to store the readings in the instrument buffer and then download them to the personal computer after completing the voltage measurements. Moreover, for the digital multimeters it was found the timing was more repeatable if the voltage range was specified in advance rather than using the default setting of "auto-voltage range." Using a GPIB trigger was found to be greatly superior to simply sending a command to start storing readings. An external trigger might be even better, but the GPIB general executive trigger (GET) was found to be convenient and adequate for the present purpose.

Figure 5 shows an example of the measured voltages across the reference resistor. The result is qualitatively identical for the voltage across the hot wire. If the timing is correct, the reading at $t = 0$ should be half of that of the second voltage reading. This

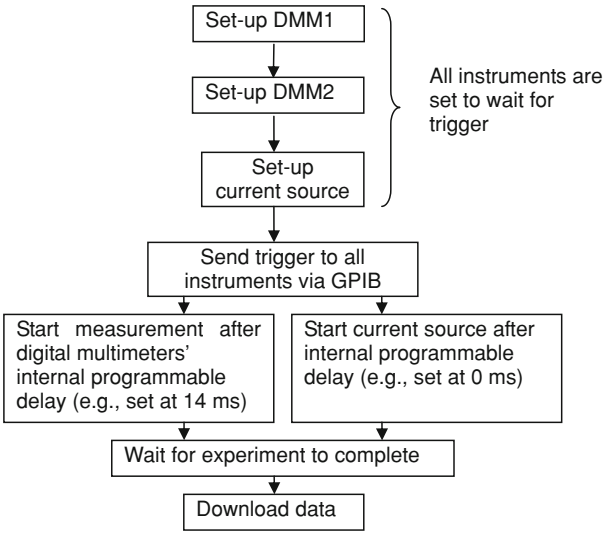

Fig. 4 Procedure for synchronizing current source and multimeters

arises from the principle that for a step rise in voltage from 0 to a fixed value, only half of the integration period for the multimeter should cover the fixed voltage if the integration period is centered at $t = 0$. The multimeters and the current source have programmable delay times to start measuring after receiving the trigger command. By adjusting the delay times by trial and error, the timing shown in Fig. 5 was achieved. Noting that the integration time is one power-line cycle (NPLC = 1) (i.e., 16.67 ms for 60 Hz power), it can be calculated that the timing in Fig. 5 is still in error by about −0.49 ms. This error can be corrected using the following formula:

$$t_{\text{true}} = t_{\text{multimeter}} + \left(\frac{V_{\text{reading1}}}{V_{\text{step}}} - \frac{1}{2} \right) \times \Delta t_{\text{integration}} \tag{7}$$

In Eq. 7 t_{true} is the time where zero corresponds to half the rise of the step and $t_{\text{multimeter}}$ is the time where zero corresponds to the first reading in the buffer of the multimeter. $\Delta t_{\text{integration}}$ is the integration time (16.67 ms for NPLC = 1). The main requirements of Eq. 7 are that the voltage step occurs within the integration time for the measurement and the integration time is accurate and weighted uniformly. Using this procedure, it is estimated that the timing for the digital multimeters is correct within ±0.1 ms.

5 Measurement of Initial Resistance

In order to determine the transient temperature rise, it is essential to be able to measure accurately the initial resistance of the unheated wire. For the conventional hot-wire method applied to low thermal-diffusivity fluids, the initial resistance is important for thermal-diffusivity measurement and for determining the bath temperature. The thermal conductivity is not affected greatly since it is determined based on the slope

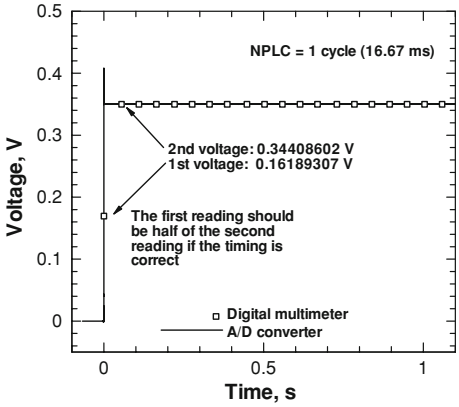

Fig. 5 Voltage measurements across the reference resistor

of the curve. However, for high thermal-diffusivity gases and for the steady-state hot-wire method, the initial resistance can affect the thermal-conductivity measurement directly. In this section, we discuss two possible approaches for measuring the initial resistance of the hot wire.

5.1 Use of a Small Current

A common method to measure the initial resistance is to apply an electrical current that is small enough so that the temperature rise of the wire can be neglected (e.g., Ref. [6]). Such a procedure requires very accurate voltage measurements. The digital multimeters employed in this study have a minimum full-scale setting of ±210 mV with $7^{1/2}$ digit resolution. In contrast, the 24 bit A/D converter has a minimum full-scale setting of ±1 V with $6^{1/2}$ digit resolution. Also, within the instrument specifications the A/D converter has a 2σ uncertainty of 50 μV + 0.05 % of the input and a DC drift of at least 5 μV/°C change from the self-calibration temperature. This makes it difficult to zero the instrument with a great enough accuracy for small voltage measurements. Figure 6 shows the electrical resistance of the platinum wire measured with different currents using the different instruments. Averaging was done over a period of 120 s for the digital multimeters and 1 s for the A/D converter (at sampling rate: 50000 s^{-1}). The polarity of the current was reversed by sending a command to the current source instrument to output a negative current. For this particular test, the sample gas was hydrogen at 0.3 MPa.

The difference between the forward and the reverse polarity measurements in Fig. 6a can be explained if there is a zero error in the voltage readings of about 13 μV for the A/D converter and about 4 μV for the digital multimeter. The origin of the voltage zero error is Seebeck effects from the junctions of different materials in the circuit and in the instruments themselves. Also, an error of 13 μV is within what we may expect from the manufacturers' specifications for the DC drift of the A/C converter (5 μV/°C change from the self-calibration temperature). It should be mentioned here that considerable effort was made to try to reduce Seebeck effects in the circuit using

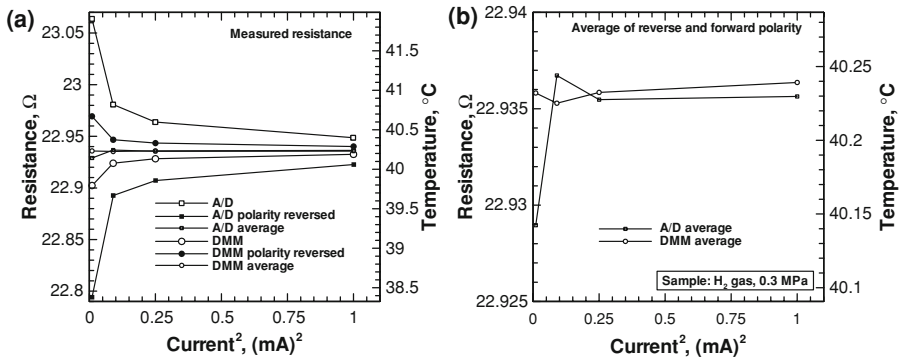

Fig. 6 Effect of changing polarity when measuring initial resistance with a small current (A/D = analog/digital converter, DMM = digital multimeter)

platinum connecting wires and thermally insulating pairs of junctions of dissimilar metals in the circuit. In spite of this, Fig. 6a still shows sensitivity to the polarity of the current. Also, we found it is important to occasionally rerun the self-calibration program for this particular A/D converter.

It is quite clear from Fig. 6a that if we want to use a current less than 1 mA, then we need to use the average of the resistances measured with forward and reverse polarities. Alternatively, we suppose that (in principle) zero errors due to Seebeck effects could be reduced by subtracting an accurate measurement of the initial voltage readings before applying any current. For the present data, failure to consider such effects could result in an error larger than 0.2 K in the measured temperature rise for the case of the A/D converter in Fig. 6. In any case, reversing the current polarity is a useful test. Fortunately, as mentioned above, the polarity of the current source can be changed automatically by computer through a simple software program without any alteration to the circuit wiring. Figure 6b shows the averages of measured resistances. For currents less than 0.5 mA, the resistance measurements appear less reliable. For 0.5 mA and 1 mA, there is a discrepancy of the order of 0.01 K between the two instruments. Moreover, as expected, the A/D converter is inferior to the digital multimeter for measuring the initial resistance with a small current.

5.2 Initial Resistance by Extrapolation from Larger Currents

Because of the large difference between the forward and the reverse polarity measurements shown in Fig. 6a, we decided to explore the possibility of using larger currents and then extrapolating to zero to obtain the initial resistance. This procedure has the advantage that the resistance can be measured much more accurately with a large voltage than with a small voltage. This is particularly true for the A/D converter. Also, the repeatability was found to be better than using a small current. The disadvantage is that the theory required for extrapolation to zero is not exact since properties of the wire and surrounding sample change with temperature (and therefore with time also).

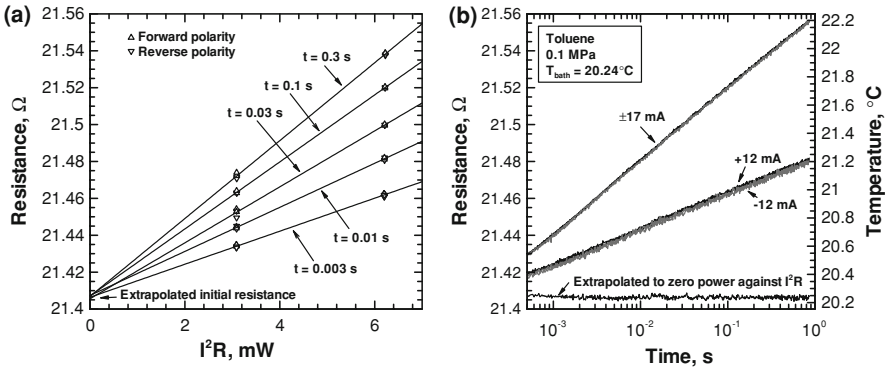

Fig. 7 Measured and extrapolated resistances for hot wire in a toluene sample. **(a)** Against power and **(b)** against time

A brief discussion of the theoretical basis for extrapolating to find the initial resistance is given in the Appendix.

Figure 7 shows an example of the extrapolation to find the initial wire resistance based on resistance measurements using a 12 mA current and a 17 mA current where the sample is toluene. Both forward and reverse polarities were used in the extrapolation, the experiment being repeated eight times (17 mA, −17 mA, 12 mA, −12 mA, 17 mA, −17 mA, 12 mA, −12 mA) using computer control with 15 s between each measurement (c.f. Fig. 2a). Generally, the resistance measured with reverse polarity appeared slightly smaller than the corresponding resistance measured with forward polarity. However, the effect of the polarity on the resistance measurement is greatly diminished from that shown in Fig. 6a for small currents.

Figure 7b shows the initial resistance estimated by extrapolation at instantaneous points in time throughout the duration of the experiment. While only one value is needed for the initial resistance, the plot in Fig. 7b has proven to be a useful test of the quality of the experimental data. If the values of the initial resistance (estimated from extrapolation) change with time, then there may be something wrong with the data. Moreover, invariance with time is one indication of the validity of the extrapolation procedure itself. Note that in Fig. 7b less than 10 % of the 50,000 data points are shown for the sake of reducing memory requirements for the soft-copy version of the figure.

To test the validity of the present extrapolation method theoretically, two-dimensional numerical simulations were done using the finite-volume method (see Ref. [2] for details of the numerical procedure used). For the purpose of simulation, rather than using a constant value for q in Eq. 3, a constant current was assumed and the resistance of the wire was taken to vary linearly with temperature (Eq. 1). Thus, q at local points in the wire varied with time and position corresponding to the local temperature. Simulations were done for both hydrogen and toluene including the temperature dependence of the fluid thermal conductivity and thermal diffusivity. For toluene, fluid properties varied with temperature according to the reference data by Watanabe [17]. Figure 8 shows the results of the simulation for toluene. A close correspondence between the experiment (Fig. 7) and the simulation (Fig. 8) should be

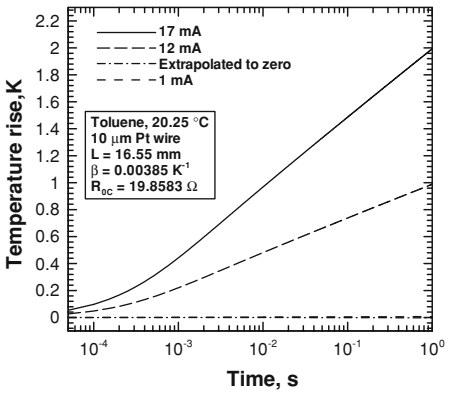

Fig. 8 Simulation of the temperature rise and extrapolation to find initial resistance for conditions similar to those in Fig. 7

expected since the length of the Pt wire was decided based on results for toluene at similar conditions to those shown in Fig. 8.

The key point of interest in Fig. 8 is the theoretical validity of using either a small current (1 mA) or extrapolating from the two larger resistance measurements to obtain the initial resistance of the hot wire. Since we are interested in the temperature rise, the initial resistance of the wire at the bath temperature was subtracted from the extrapolated initial resistance estimates and the result was expressed as a "temperature rise" in Fig. 8. Based on the results in Fig. 8, the theoretical error in the initial temperature measurement by extrapolation is less than about 2 mK over the duration of the 1 s experiment for these conditions. The 1 mA current measurement on the other hand leads to a temperature rise in the hot wire of about 7 mK at $t = 1$ s. This is shown more clearly in Fig. 9a which includes the extrapolated data from Fig. 8 on an enlarged scale. From Fig. 9a it is apparent that the extrapolation tends to underestimate the initial resistance, while using a small current gives an overestimate. In the case of hydrogen (not shown), however, extrapolation overestimates the initial resistance by 1.6 mK at $t = 1$ s (using 15 mA and 10 mA currents). Reducing the current from 1 mA to 0.5 mA leads to a reduction of the error to one quarter. This should be expected since the temperature rise is approximately proportional to the square of the current. Clearly from Fig. 9a, extrapolating against I^2R is better than extrapolating against I^2. The error in the extrapolation is related to both the change in resistance of the wire with temperature and the change in the properties of the fluid with temperature. Figure 9b shows the results of a simulation with the fluid properties held constant. As should be expected, the extrapolation error becomes smaller if the properties are held constant. In particular, extrapolation against I^2R gives a very small error. Extrapolation from a current smaller than 12 mA will result in an error smaller than that shown in Fig. 9a. A compromise has to be reached between the accuracy at which the resistance can be measured and the loss in accuracy through extrapolation. Nevertheless, Fig. 9a demonstrates that a current as large as 12 mA (about two thirds of the measuring current) can be used as a basis for extrapolation.

Figure 10a compares the initial resistance for the wire in a toluene sample measured using the digital multimeters and the A/D converter as a function of time. The black line shows the result of extrapolation already plotted in Fig. 7b but on an enlarged

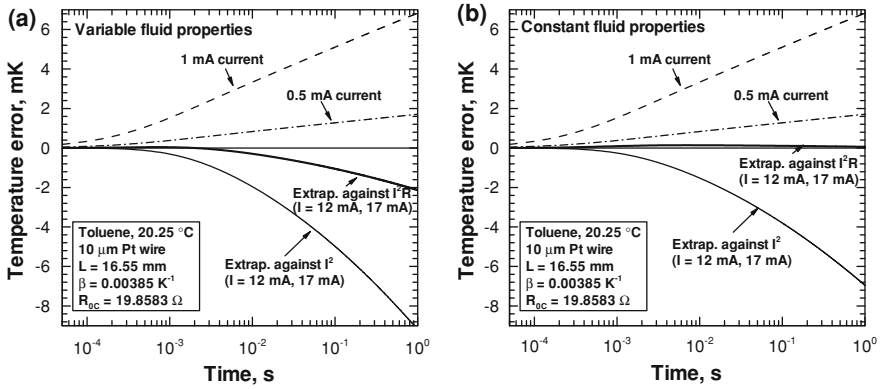

Fig. 9 Simulated error in the initial resistance measurement (expressed in terms of temperature) from either extrapolation or using a small current. **(a)** Variable fluid properties and **(b)** constant fluid properties

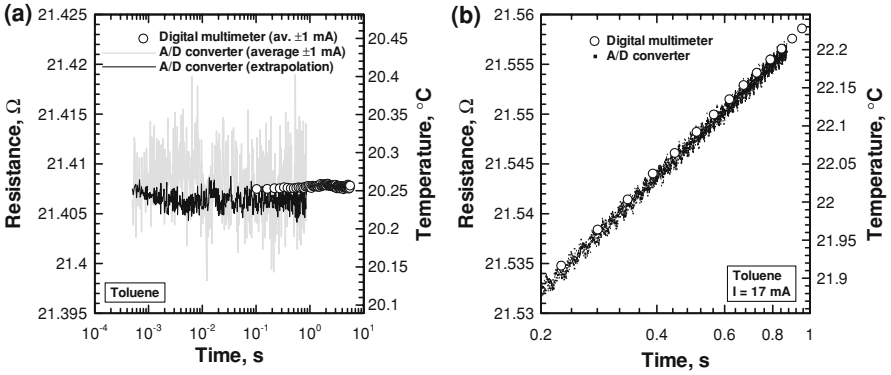

Fig. 10 Resistance of the hot wire in toluene sample. **(a)** Initial resistance measurement and **(b)** resistance for 17 mA

scale. The gray line and the circles are resistances measured with using a 1 mA current with the A/D converter and digital multimeter, respectively. The black line shows considerably less scatter than the gray line indicating an improvement to the precision of the measurement as a result of using extrapolation rather than a small current. In this particular case, the time average of the estimated initial resistance using the digital multimeter (21.4077 Ω, 20.255 °C) is in very good agreement with that using the A/D converter (21.4079 Ω, 20.256 °C). On the other hand, extrapolation gives an average initial resistance of 21.4063 Ω, 20.236 °C which is 20 mK lower than the values measured with ±1 mA current. Of this 20 mK discrepancy, up to about 9 mK can be explained based on the simulation shown in Fig. 9a. The remainder must be attributed to other experimental uncertainties. It is worth pointing out that the digital multimeter readings are about 10 mK higher than the A/D converter readings for the 17 mA current case shown in Fig. 10b. Therefore, the influence of this difference on the actual temperature rise is less than 20 mK.

6 Measurement Noise Reduction

Comparing the A/D converter data with the digital multimeter data in Fig. 10a, it is obvious that the integrating multimeter has superior noise rejection characteristics. Nonetheless, the noise in the A/D converter data shown in Figs. 2b, 7b, and 10b is remarkably low in spite of the high sampling rate of 50000 s^{-1}. Therefore, it is worthwhile explaining how this result was achieved. Figure 11 shows three different possible ways (Fig. 11b–d) of determining the transient resistance from the raw data (Fig. 11a). For the case shown in Fig. 11b, the time average of the electrical current (14.0005 mA) was used to convert the voltage across the platinum wire (Fig. 11a) into the resistance. This is simply a rescaling of the vertical axis of Fig. 11a, so the relative level of noise is the same for Fig. 11a, b. From a careful examination of Fig. 11a, it is apparent that there is a correlation between the "noise" in the measured current and the "noise" in the measured voltage across the hot wire. We believe this is not simply common-mode noise between sampling cables of the two channels of the A/D converter but rather it is due to actual fluctuations of the current in the circuit. This conclusion is supported by Fig. 11c. The effect of using the instantaneous measured current rather than the time average of the measured current to calculate the resistance is dramatic. It can be seen by comparing Fig. 11b with c.

Figure 11c shows one of the curves previously shown in Fig. 2b. Figure 11d shows the ensemble average of the four curves for ± 14 mA given in Fig. 2b. From Fig. 11d, we can conclude that ensemble averaging not only removes the effect of thermal emfs in the circuit but also reduces the random noise. Taking ensemble averages of more than four measurements results in a greater noise reduction, but for the present purpose, four measurements appear to be adequate. It is worth mentioning here that the present approach may be considered as an alternative to conventional filtering (e.g., Ref. [9]) which has the advantage of a simpler experimental procedure.

To confirm our interpretation that the high-frequency oscillations in the electrical current trace shown in Fig. 11a are actual fluctuations in the current in the circuit, we carried out a simple experiment with the A/D converter, two reference resistors (10 Ω and 100 Ω), and a high-frequency signal generator. The circuit was set-up in the same way as shown in Fig. 1 except that the current source was replaced by the signal generator and the hot wire was replaced by a four-terminal 10 Ω reference resistor of a similar type to that used in the hot-wire experiment. The signal generator was set to output a small amplitude (0.01 Vpp) high-frequency oscillation (20 kHz) with a DC offset of 0.4 V. The frequency of 20 kHz was selected because it is of a similar order to the apparent noise in Fig. 11a. Moreover, it is approaching the Nyquist limit (25 kHz) for an ideal instrument sampling at 50 kHz. The system was then used to measure the resistance of the 10 Ω reference resistor in the same way that the resistance of the hot wire is measured. Figure 12 shows the results. The regularity in the oscillations indicates that they are certainly due to the 20 kHz output from the function generator (i.e., the high-frequency oscillating current in the circuit). The sine-wave shape is not so clear because the sampling rate of 50 kHz is not fast enough. The improvement to the measured resistance using the instantaneous current rather than the time-averaged current is obvious from a comparison of the square symbols with the black circle symbols. We also tested the frequency response of the reference resistor using a lock-in

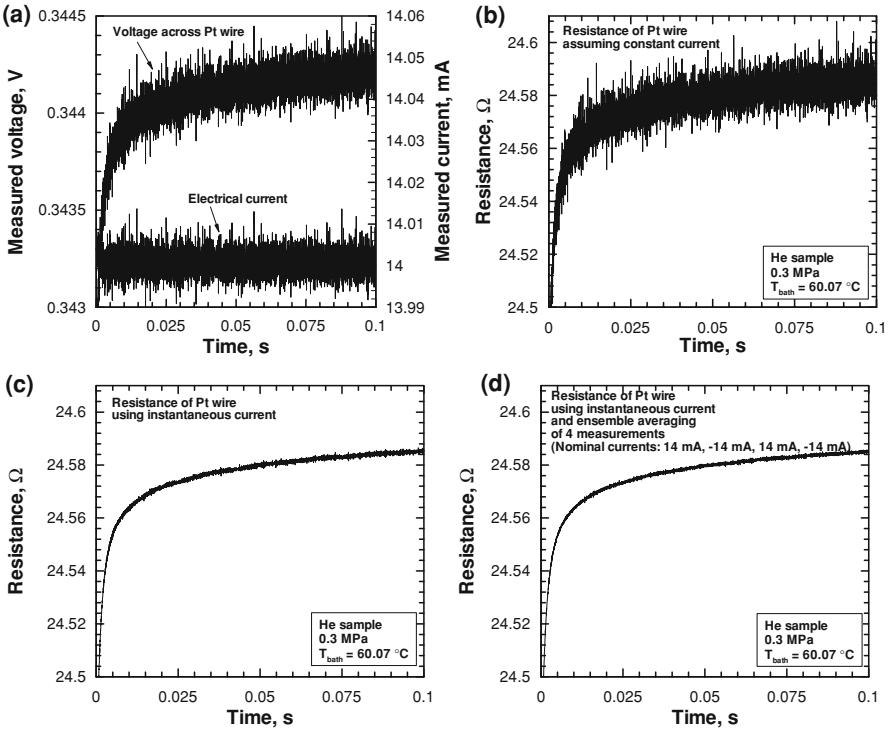

Fig. 11 Different ways of determining the transient resistance. **(a)** Measured voltage and current, **(b)** resistance assuming a constant current, **(c)** using instantaneous current, and **(d)** ensemble averaging of four measurements (recommended)

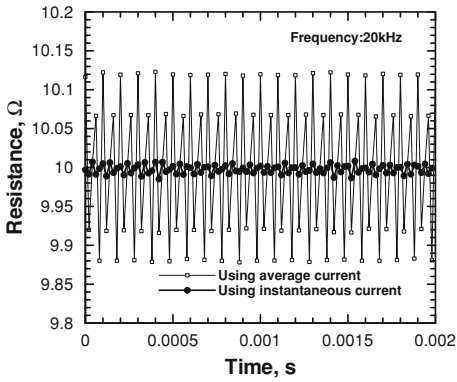

Fig. 12 Demonstration that the A/D converter system can respond to high-frequency currents in the circuit

amplifier. It was found that it behaved like an ideal DC resistance within ±0.5 % up to a frequency of 100 kHz. This confirms that our system is capable of responding to high-frequency fluctuations in the electrical current.

While Fig. 12 gives an indication of the system capabilities, it does not prove that the correlation in the noise in Fig. 11a is due to noise in the output current from the

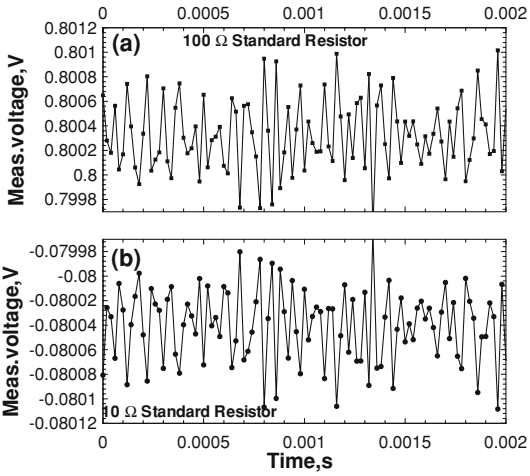

Fig. 13 Measured voltages for circuit containing two standard resistors. **(a)** 100 Ω and **(b)** 10 Ω

current source. However, a close examination of the noise in the circuit using two reference resistors (10 Ω and 100 Ω) supports our interpretation. Figure 13 shows the output voltages from the two channels where the same system shown in Fig. 1 is used except that the hot wire is again replaced by a 10 Ω reference resistor and the 25 Ω resistor is replaced by a 100 Ω resistor. In the same manner as in the hot-wire experiment, the channels of the A/D converter are connected in opposite polarity to avoid a ground-loop error (c.f. Fig. 3). If the correlated noise was from within the A/D converter itself we would expect that the noise on channel 0 would be in phase with the noise on channel 1. On the other hand, if the noise is in the current flowing through the circuit, then it should be 180° out of phase because of the opposite polarity of the connections of the two channels. Figure 13 shows that the correlated noise for the two channels is in fact 180° out of phase (Fig. 13a is roughly a vertical mirror image of Fig. 13b). Moreover, the vertical scale on Fig. 13a is set at ten times that of Fig. 13b. This shows that the amplitude of the correlated noise is in proportion to the magnitude of the resistor. This is further evidence that the correlated noise is related to a noisy output current from the current source.

7 Instrument Calibration for Thermal-Conductivity Measurements

Unlike the conventional transient hot-wire method, which is usually an absolute method, the transient *short*-hot-wire method may be considered a kind of relative method. It is 'relative' in the sense that the geometry of the wire used in the model is decided based on measurements taken in a reference fluid of known thermal conductivity and thermal diffusivity [6,7]. This is a very convenient and practical way to determine the wire length and diameter, and for short wires it generally result in more accurate thermal-conductivity measurements than can be achieved by direct measurements of the geometry using microscopes. One reason for this is that the wire is so short that small uncertainties about the precise location of the weld attachment

Table 1 Calibrated effective geometry by different voltmeters (with toluene, 21.38 °C)

Method to measure R_0	A/D converter				Digital multimeters			
	Extrapolation		Small current (±1 mA)		Extrapolation		Small current ±1 mA	
Run No.	L (mm)	d(μm)	L (mm)	d(μm)	L (mm)	d(μm)	L (mm)	d(μm)
1	16.59	9.88	16.58	10.36	16.59	9.86	16.59	10.02
2	16.56	9.93	16.58	10.32	16.58	9.90	16.57	10.08
3	16.59	9.84	16.55	10.42	16.61	9.83	16.60	10.03
Average	16.58	9.88	16.57	10.37	16.59	9.86	16.59	10.04

positions may correspond to a significant fraction of the measured wire length. The effect of differences between the model and the actual cell geometry also may be improved through calibration.

For this study, we calibrated our instrument using liquid toluene. Toluene has been recommended as one of the international standard reference fluids for calibrating thermal-conductivity instruments [18]. It has an estimated 2σ uncertainty of about ±0.6 % at 25 °C, 0.1 MPa and ±1 % over a wide temperature range. Therefore it is desirable to be able to link other fluid thermal conductivities to this standard. The thermal conductivity is of the same order of magnitude as that of low-density helium gas although the thermal diffusivity is different by several orders of magnitude. The reference value for the thermal diffusivity of toluene was taken from Watanabe [17]. The toluene used had a purity specified by the manufacturer of 99.8 %. No extra purification measures were taken. Table 1 shows the result of the calibration.

Three different measurements were taken at bath temperatures of 20.24 °C, 20.23 °C, and 20.23 °C with a final temperature increase of about 1.9 K (reference temperatures for A/D converter were 21.37 °C, 21.37 °C, and 21.38 °C following the recommendation for the effective fluid temperature given in Ref. [1]). We can see from Table 1 that the average calibrated effective lengths for the four different methods agree within about 0.1 %. The diameter is sensitive to the method used for determining the unheated wire resistance, R_0. For the case of the A/D converter, d is 5 % larger if estimated using a small current rather than extrapolation to determine the initial wire resistance R_0. On the other hand, both the diameter and the length are in excellent agreement for both the A/D converter and the digital multimeter if extrapolation is used to determine the initial wire resistance. This is another motivation for using extrapolation rather than a small current.

8 Uncertainty Analysis

Because of the use of the numerical solution, the uncertainty analysis for the transient short-hot-wire method is somewhat complicated. Following the general approach and notation of the ISO guideline [19], the thermal conductivity can be expressed as:

$$\lambda = f\,(X_1, X_2, \ldots, X_N) \tag{8}$$

where $f()$ is calculated by the curve-fitting method outlined in Sect. 3 above and $X_1, X_2, \ldots, X_N$ are input parameters such as measured voltages, wire diameter, wire length, properties of the wire, values of time, etc. The combined standard uncertainty $u_c(\lambda)$ is given by:

$$u_c^2(\lambda) = \sum_{i=1}^{N} \left(\frac{\partial f}{\partial x_i} \right)^2 u^2(x_i) + 2 \sum_{i=1}^{N-1} \sum_{j=i+1}^{N} \frac{\partial f}{\partial x_i} \frac{\partial f}{\partial x_j} u(x_i, x_j) \tag{9}$$

where $u^2(x_i)$ is the estimated variance of x_i (the input estimate for X_i) and $u(x_i, x_j)$ is associated with the covariance of different input quantities as explained in [19]. Since Eq. 8 cannot be differentiated analytically (see Ref. [19], Sect. 5.1.3) we made use of

$$\frac{\partial f}{\partial x_i} u(x_i) = \frac{1}{2} \{ f[x_1, \ldots, x_i + u(x_i), \ldots, x_N] - f[x_1, \ldots, x_i - u(x_i), \ldots, x_N] \} \tag{10}$$

To simplify the analysis, each of the voltmeters was modeled using the following equation:

$$v = v_{\text{fixed}} + v_{\text{drift},j} + B v_{\text{meas}} \tag{11}$$

where v_{meas} is a voltage reading, B is the linear coefficient with an expected value of 1, v_{fixed} is the zero error of the voltmeter at the start of the experiment (expected value 0), and $v_{\text{drift},j}$ (expected value 0) is the small change in the zero error as the experiment progresses. $v_{\text{drift},j}$ is also assumed to account for the very slight nonlinearities in the voltmeter associated with measurements at different voltages. For the present experiment, $v_{\text{drift},j}$ is taken to be a separate constant for each of the eight electrical currents used ($j = 1, 8$) (c.f. Fig. 2). Equation 11 was not used to correct the voltage (since the expected values of the zero error and drift were taken to be zero) but rather as the tool for including the uncertainties. By assuming that Eq. 8 accounts for all correlations between different voltage measurements using the same instrument and that all quantities on the right-hand side of Eq. 8 are uncorrelated, then Eq. 9 may be simplified to

$$u_c^2(y) = \sum_{i=1}^{N} \left(\frac{\partial f}{\partial x_i} \right)^2 u^2(x_i) \tag{12}$$

Note that we have also assumed that all other input quantities are uncorrelated. Equation 10 is evaluated by perturbing a single input quantity, and then the thermal conductivity is reevaluated using the curve fitting procedure. For the A/D board with 50,000 voltage readings it is impractical to use Eq. 10 for each voltage input. Instead, Monte Carlo simulations (50 calculations of λ) were done to evaluate the combined uncertainty associated with individual voltages and also $v_{\text{drift},j}$ in Eq. 11.

Table 2 Uncertainty analysis (1σ standard uncertainties)

	A/D converter		Digital multimeters	
	$u(x_i)$	Effect on λ (%)	$u(x_i)$	Effect on λ (%)
Voltmeter zero (excluding drift)	25 μV	0.0005	0.9 μV	0.06
Voltmeter drift/shift (with t and v)[a]	4 μV	0.4	0.02 μV	0.002
Voltmeter linear coefficient	0.025 %	0.05	0.001 %	0.002
Voltmeter precision[a,b]	50 μV	0.02	1.9 μV	0.094
Bath temperature stability	0.008 K	0.4	0.008 K	0.4
Starting time	0.05 ms	0.01	0.05 ms	0.001
Wire diameter	1.6 %	0.24	1.4 %	0.22
Wire length	0.5 %	0.43	0.5 %	0.43
Cell diameter	0.3 mm	0.004	0.3 mm	0.004
Platinum thermal conductivity	1.5 %	0.01	1.5 %	0.01
Platinum heat capacity (ρc)	2.5 %	0.008	2.5 %	0.001
Combined uncertainty (%)		0.76		0.65

[a] Effect of uncertainty on λ estimated from Monte Carlo simulations
[b] Single reading using present instrument settings without additional filtering

It is worth mentioning that the correlation between the two channels of the A/D converter observed in Sect. 6 above was also considered by a Monte Carlo simulation. However, its effect on the measured thermal-conductivity uncertainty was found to be insignificant.

Table 2 shows the results of the uncertainty analysis. The estimated standard uncertainties for the wire length and diameter were calculated using the uncertainties for toluene properties given by Ramires et al. [18] for thermal conductivity (±1 % with $k = 2$) and Watanabe [17] for thermal diffusivity (±4 % with $k = 2$). The four quantities related to the voltmeter in Table 2 correspond to the four quantities on the right-hand side of Eq. 11. These uncertainties were estimated based on the manufacturers' specifications of each instrument. The analysis shows that in spite of the large uncertainty in the voltmeter zero for the A/D converter (25 μV) the effect on λ is small. This can be attributed to the effectiveness of reversing the polarity in the measurement. On the other hand, because the present extrapolation procedure requires measurements with several different currents, any drift in the bath temperature or in the instrument zero can make a contribution to the uncertainty in the thermal-conductivity measurement. Finally, based on Table 2, the thermal-conductivity measurements are estimated to have an expanded uncertainty of 1.5 % for the A/D converters and 1.3 % for the digital multimeters where the coverage factor, k, is 2.

9 Thermal-Conductivity Measurement Results

Figure 14 gives a comparison of the results of the least-squares fitting procedure using the data collected by the A/D converter (Fig. 14a) and the digital multimeters

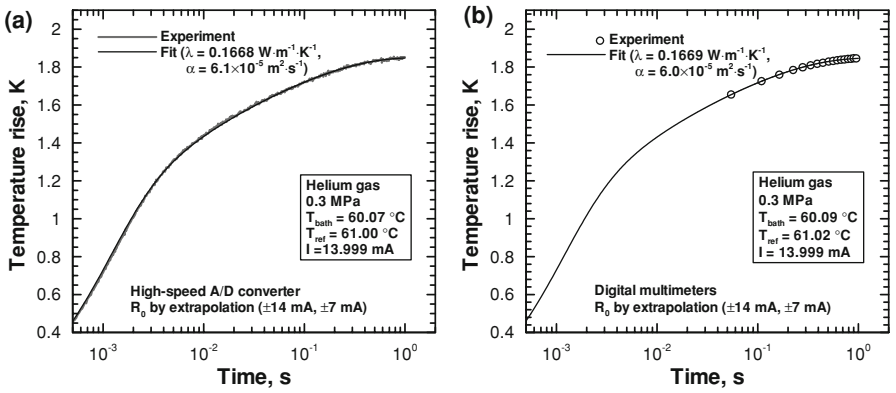

Fig. 14 Volume-averaged temperature rise of the platinum wire

(Fig. 14b). The sampling rate for the digital multimeters was 15 s^{-1}, while for the A/D converter, 50000 s^{-1} was used. The integration period for the digital multimeters was set at 1 power line cycle (16.67 ms). The experimental data are in excellent agreement with the shape of the curve calculated using Eqs. 2–6. For $t > 0.01$ s in Fig. 14a, almost all the experimental points are within ±1 % of the calculated curve (standard deviation of 0.26 %). The largest deviation (about −3 %) is for $t < 0.001$ s. Data for times less than 0.5 ms were not included in the fitting procedure due to an apparent influence of the overshoot shown in Fig. 3. For the case of the digital multimeters (Fig. 14b), all 15 measurements are within ±0.1 % of the calculated curve (standard deviation of 0.043 %).

The surprising result from Fig. 14 is that both the high-speed A/D converter (50000 s^{-1}) and the digital multimeters (only 15 s^{-1}) gave almost the same thermal conductivity for the sample (0.1668 $W \cdot m^{-1} \cdot K^{-1}$). This value deviates by about 0.7 % from the dilute-gas correlation by Hands and Arp [20] (0.1680 $W \cdot m^{-1} \cdot K^{-1}$) and also from the result calculated by Hurly and Moldover [21] [0.1678 $W \cdot m^{-1} \cdot K^{-1}$ (interpolated from their tabulated values)]. The pressure dependence of the helium thermal conductivity at 0.3 MPa, 61 °C is very small resulting in a change of about 0.07 % from the dilute gas value based on the measurements of Assael et al. [22]. The thermal diffusivities in Fig. 12 are about 20 % lower than that expected from reference values for the density and specific heat capacity [23,24] (7.50×10^{-5} $m^2 \cdot s^{-1}$). This may be attributed to the imperfect representation of the geometry of the domain and other experimental errors.

For the case shown in Fig. 14, the initial resistance of the wire R_0 was determined by extrapolation to zero power using the transient resistance measured with two different nominal electric currents (±7 mA and ±14 mA). Using a small current (±0.5 mA) to measure the initial resistance was also successful for helium gas. Figure 15 shows measurements of helium thermal conductivity at nominal temperatures of 20 °C, 40 °C, 60 °C, and 80 °C. Figure 15a, b shows the results for the high-speed A/D converter, while Fig. 15c, d is for the pair of digital multimeters. In Fig. 15a, c extrapolation was used to determine the initial resistance, while in Fig. 15b, d a small

Table 3 Measured helium thermal conductivity at 0.3 MPa

Instrument	T_{ref} (°C)	$\lambda(W \cdot m^{-1} \cdot K^{-1})$	2σ uncertainty (%)
High-speed A/D converter	21.11	0.1514	1.5
	41.19	0.1591	
	61.00	0.1669	
	80.81	0.1746	
Digital multimeters	21.12	0.1514	1.3
	41.20	0.1591	
	61.02	0.1669	
	80.84	0.1745	

current was used. For the cases of the extrapolated initial resistance (Fig. 15a, c) the experiment was repeated six times. Table 3 gives the average thermal conductivities corresponding to Fig. 15a, c. For the cases shown in Fig. 15b, d, the experiment was only done twice at three nominal temperatures. The initial resistance is the average of both forward and reverse polarities. From Fig. 15, we may conclude that it is possible to use either extrapolation or a small current to determine the initial resistance for measurement of low-pressure helium thermal conductivity.

It should be emphasized here that the "fit" shown in Fig. 15 was not decided by the judgment of the experimentalist but by a mathematical procedure described in [2]. The curve-fitting procedure requires that Eq. 2 be solved a number of times to determine λ and α from Eq. 6. Thus the scatter (or lack of scatter) in Fig. 15 is a true reflection of the precision of the technique. Consistent with Fig. 14, a comparison of Fig. 15a, c shows that the precision of measured thermal conductivity is similar using either the high-speed A/D converter (about ± 0.3 %) or the pair of digital multimeters (about ± 0.4 %). Note that this precision is based on measurements taken on the same day and corresponds to two standard deviations. In the case of another gas (hydrogen), repeating measurements a few months later led to a shift in the average by about 0.6 % for the nominal temperature of 60 °C.

The dashed line in Fig. 15 is the dilute-gas thermal conductivity correlation by Hands and Arp [20], while the solid line is the same result plus a small correction for the density dependence of the thermal conductivity. For this correction, the excess thermal conductivity from the measurements of Assael et al. [22] was used. At a pressure of 0.3 MPa, this correction is smaller than the uncertainty in the experimental data. Hurly and Moldover [21] reported *ab initio* quantum mechanical calculations of helium thermal conductivities which are also shown in Fig. 15. For the temperature range shown in Fig. 15, both the correlation by Hands and Arp and the calculations by Hurly and Moldover are in agreement with experimental data by Assael et al. [22], Kestin et al. [25], Mustafa et al. [26], and Hemminger [27] within ± 1 %. The present results given in Fig. 15 show a small systematic deviation in the trend of the temperature dependence of the helium thermal conductivity when compared with the reference data. The largest deviation from the reference data is at the nominal temperature of

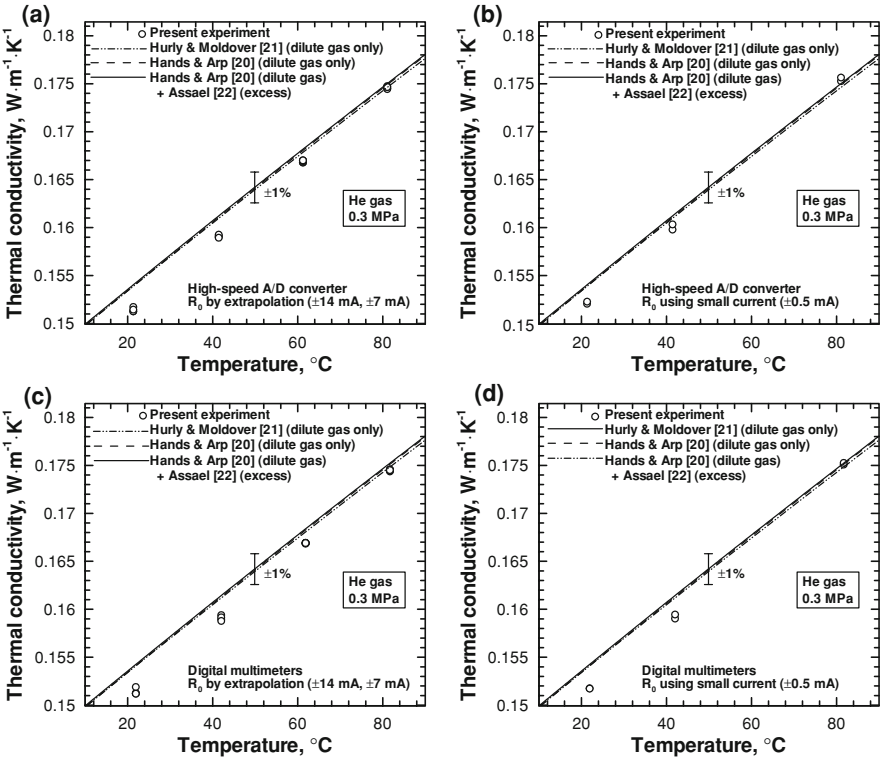

Fig. 15 Helium-gas thermal conductivity using different voltmeters and different methods for determining the initial unheated wire resistance. **(a)** High-speed A/D converter with initial resistance by extrapolation, **(b)** high-speed A/D converter with initial resistance using a small current, **(c)** digital multimeters with initial resistance by extrapolation, and **(d)** digital multimeters with initial resistance using a small current

20 °C, where the present results are about 1.6 % lower than the correlation of Hands and Arp [20]. This is slightly outside of the estimated uncertainty of our measurements. Therefore, based on the reported high accuracy of the reference data for helium in this range of temperature and pressure [21,22,25–27], we suppose that there may be a small unknown systematic effect that has not been included in our analysis. The close agreement between the results of the two instruments shown in Table 3 suggests that the problem is probably not with the voltage measurement instrument. Moreover, the DC voltage drift for the A/D converter may be less than that estimated in Table 2 based on the manufacturer's specifications.

10 Conclusion

The thermal conductivity of low-pressure helium gas can be measured accurately by the transient short-hot-wire method with either a two-channel high-speed A/D converter or a pair of integrating digital multimeters. The digital multimeter has the disadvantage that few data points are available at small values of time. Also, more effort is

required to synchronize the instruments. On the other hand, the A/D converter faces the challenge of measuring the initial resistance of the platinum hot wire accurately enough. It was found that the noise in the transient resistance measurement by the A/D converter can be reduced through using an instantaneous current measurement rather than an average current measurement. For either type of instrument, it is important to confirm and remove the effect of reversing the polarity of the current source. All the practical issues discussed in this article are expected to be more important for low-density, high thermal-diffusivity gases than for liquids and high-pressure gases.

Acknowledgment This research has been conducted as a part of the "Fundamental Research Project on Advanced Hydrogen Science" funded by the New Energy and Industrial Technology Development Organization (NEDO).

Appendix: Theoretical Basis for Extrapolation to Find Initial Resistance of Hot Wire

Although it is not used in this study, the usual working equation (e.g., Ref. [1]) for the transient hot-wire method is suitable for outlining a theoretical basis for the extrapolation procedure proposed in Sect. 5.2 above. The basic equation (without any corrections) is

$$T = (q/(4\pi\lambda)) \ln\left(4\alpha t/\left(r_0^2 C\right)\right) \tag{A1}$$

where T is the temperature rise of the wire, q is the power per unit length, and C is a constant. From this equation, we should expect that at a constant time, t, for different experiments, the temperature rise will be proportional to the power, q, i.e.,

$$T = K(t)\, q \tag{A2}$$

where K is a constant for a fixed value of t from different ensemble experiments. Suppose we have $q = I^2 R/L$ (where I is the electrical current) and a linear relation for the resistance of the wire as follows:

$$R = R_{0C}(1 + \beta(T_{\text{initial}} + T)) \tag{A3}$$

where R_{0C} is the resistance at 0 °C, β is the temperature coefficient of resistance and T_{initial} is the initial temperature of the wire in °C (i.e., bath temperature). Let R_{initial} be the resistance of the unheated wire at the temperature, T_{initial}. Then,

$$R = R_{\text{initial}} + R_{0C}\beta T \tag{A4}$$

Substituting Eq. A2 for T gives

$$R = R_{\text{initial}} + R_{0C}\beta K(t) q \tag{A5}$$

For this ideal case, since $R_{0C}\beta K(t)$ is a constant for different experiments at a given time t, we may find the initial resistance R_{initial}, by extrapolating to zero against different powers, q, i.e., against different values of I^2R at fixed values of time from different experiments. The question that needs answered is whether or not other secondary effects (i.e., corrections to the ideal equation, such as variable fluid properties, the change in q with time, temperature jumps, radiation, and natural convection) cause such an extrapolation to lose accuracy. We have already discussed the validity of the extrapolation procedure in relation to the change in the wire resistance, R, with time and variable fluid properties (Sect. 5.2; Figs. 8, 9).

For temperature jumps, Healy et al. [28] give an expression where the temperature jump is proportional to the power, q;

$$\delta T_{\text{jump}} = (q/4\pi\lambda)\,(2g/r_0) \tag{A6}$$

In Eq. A6, g is an empirical factor proportional to the mean free path and δT_{jump} is the temperature discontinuity at the wire surface. Therefore, if the Eq. A6 result is justifiable, then the above reasoning still applies for the case of a temperature jump since correcting Eq. A2 results in an instantaneous temperature rise that is proportional to the power.

For radiation, Healy et al. [28] linearize the radiation loss as follows:

$$q_{\text{rad}} = 2\pi r_0\sigma\left(T_{\text{w}}^4 - T_{\text{initial}}^4\right) \approx 8\pi r_0\sigma T_{\text{initial}}^3 T \tag{A7}$$

where σ is the Stephan–Boltzman constant, T_{w} is the wire temperature, and T is the temperature rise of the wire. The temperature of the wall is assumed to be the same as the initial temperature of the wire and the fluid is taken to be thermally transparent. If we subtract the linearized approximation for q_{rad} from q and substitute into Eq. A2, then we obtain

$$T = \frac{K(t)}{1 + K(t)\,8\pi r_0\sigma T_{\text{initial}}^3}q \tag{A8}$$

The coefficient of q in this expression is also a constant for the same bath temperature at fixed t. Therefore we may say that for the linearization of radiation recommended by Healy et al. [28], our proposed extrapolation is still reasonable. Of course, this only applies in circumstances where the linearization of radiation given in Eq. A7 is valid.

Natural convection is a further possible source of non-linearity. For example, if we tried to extrapolate to find the initial resistance based on steady-state resistances in dense fluids or after large periods of time when natural convection effects dominate, then extrapolating to zero against the power would be inaccurate. However, rather than this, we are proposing instantaneous extrapolations during the short measurement time up to 1 s, which is before natural convection effects become significant. This is consistent with another basic principle of the transient hot-wire method, i.e., that natural convection can be neglected if the time is short enough.

References

1. M.J. Assael, C.A. Nieto de Castro, H.M. Roder, W.A. Wakeham, in *Experimental Thermodynamics,* III. *Measurement of the Transport Properties of Fluids*, ed. by W.A. Wakeham, A. Nagashima, J.V. Sengers (Blackwell Scientific, Oxford, 1991), chap. 7
2. P.L. Woodfield, J. Fukai, M. Fujii, Y. Takata, K. Shinzato, Int. J. Thermophys. **29**, 1299 (2008)
3. B. Taxis, K. Stephan, Int. J. Thermophys. **15**, 141 (1994)
4. H.M. Roder, R.A. Perkins, A. Laesecke, J. Res. Natl. Inst. Stand. Technol. **105**, 221 (2000)
5. M.J. Assael, L. Karagiannidis, N. Malamataris, W.A. Wakeham, Int. J. Thermophys. **19**, 379 (1998)
6. M. Fujii, X. Zhang, N. Imaishi, S. Fujiwara, T. Sakamoto, Int. J. Thermophys. **18**, 327 (1997)
7. D. Tomida, S. Kenmochi, T. Tsukada, K. Qiao, C. Yokoyama, Int. J. Thermophys. **28**, 1147 (2007)
8. M.J. Assael, M. Dix, A. Lucas, W.A. Wakeham, J. Chem. Soc. Faraday Trans. **77**, 439 (1981)
9. H.M. Roder, J. Res. Nat. Bur. Stand. **86**, 457 (1981)
10. R.A. Perkins, H.M. Roder, D.G. Friend, C.A. Nietode Castro, Physica A **173**, 332 (1991)
11. S.G.S. Beirao, M.L.V. Ramires, M. Dix, C.A. Nietode Castro, Int. J. Thermophys. **27**, 1018 (2006)
12. B.N. Srivastava, S.C. Saxena, Proc. Phys. Soc. B **70**, 369 (1957)
13. P.L. Woodfield, J. Fukai, M. Fujii, Y. Takata, Int. J. Thermophys. **30**, 796 (2009)
14. P.L. Woodfield, J. Fukai, M. Fujii, Y. Takata, K. Shinzato, Int. J. Thermophys. **29**, 1278 (2008)
15. H.M. Roder, C.A. Nietode Castro, Cryogenics **27**, 312 (1987)
16. H. Watanabe, Metrologia **39**, 65 (2002)
17. H. Watanabe, Int. J. Thermophys. **18**, 313 (1997)
18. M.L.V. Ramires, C.A. Nietode Castro, R.A. Perkins, Y. Nagasaka, A. Nagashima, M.J. Assael, W.A. Wakeham , J. Phys. Chem. Ref. Data **29**, 133 (2000)
19. ISO/IEC Guide 98-3:2008, http://www.iso.org/sites/JCGM/GUM-JCGM100.htm
20. B.A. Hands, V.D. Arp, Cryogenics **22**, 697 (1981)
21. J.J. Hurly, M.R. Moldover, J. Res. Natl. Inst. Stand. Technol. **105**, 667 (2000)
22. M.J. Assael, M. Dix, A. Lucas, W.A. Wakeham, J. Chem. Soc. Faraday Trans. **77**, 439 (1981)
23. R.D. McCarty, V.D. Arp, Adv. Cryogenic Eng. **35**, 1465 (1990)
24. V.D. Arp, R.D. McCarty, NIST Technical Note 1334 (1989)
25. J. Kestin, R. Paul, A.A. Clifford, W.A. Wakeham, Physica **100A**, 349 (1980)
26. M. Mustafa, M. Ross, R.D. Trengove, W.A. Wakeham, M. Zalaf, Physica **141A**, 233 (1987)
27. W. Hemminger, Int. J. Thermophys. **8**, 317 (1987)
28. J.J. Healy, J.J. de Groot, J. Kestin, Physica **82C**, 392 (1976)